Weierstraß-Institut
für Angewandte Analysis und Stochastik

im Forschungsverbund Berlin e.V.

Preprint ISSN 0946 – 8633

Coupling of FEM and BEM in Shape Optimization

Karsten Eppler[1] and Helmut Harbrecht[2]

submitted: 23th May 2005

[1] Weierstraß-Institut für Angewandte Analysis und Stochastik
Mohrenstr. 39
10117 Berlin
Germany
E-Mail: eppler@wias-berlin.de

[2] Institut für Informatik
und Praktische Mathematik
Christian–Albrechts–Universität zu Kiel
Olshausenstr. 40
24098 Kiel
Germany
E-Mail: hh@numerik.uni-kiel.de

No. 1029
Berlin 2005

2000 *Mathematics Subject Classification.* 49Q10, 49M15, 65N38, 65K10, 49K20, 65T60.

Key words and phrases. shape calculus, Newton method, boundary integral equations, finite element method, multiscale methods, sufficient second order conditions.

This research has been carried out when the second author stayed at the Department of Mathematics, University Utrecht, Netherlands, supportet by the EU-IHP project *Nonlinear Approximation and Adaptivity: Breaking Complexity in Numerical Modelling and Data Representation.*

Edited by
Weierstraß-Institut für Angewandte Analysis und Stochastik (WIAS)
Mohrenstraße 39
10117 Berlin
Germany

Fax: + 49 30 2044975
E-Mail: preprint@wias-berlin.de
World Wide Web: http://www.wias-berlin.de/

Abstract. In the present paper we consider the numerical solution of shape optimization problems which arise from shape functionals of integral type over a compact region of the unknown shape, especially L^2-tracking type functionals. The underlying state equation is assumed to satisfy a Poisson equation with Dirichlet boundary conditions. We proof that the shape Hessian is not strictly $H^{1/2}$-coercive at the optimal domain which implies ill-posedness of the optimization problem under consideration. Since the adjoint state depends directly on the state, we propose a coupling of finite element methods (FEM) and boundary element methods (BEM) to realize an efficient first order shape optimization algorithm. FEM is applied in the compact region while the rest is treated by BEM. The coupling of FEM and BEM essentially retains all the structural and computational advantages of treating the free boundary by boundary integral equations.

Introduction

Throughout the last 25–30 years, optimal shape design has become more and more important in engineering applications. On the one hand, many problems that arise in structural mechanics, fluid dynamics and electromagnetics lead to the minimization of functionals defined over a class of admissible domains. On the other hand, free boundary problems can be formulated as shape optimization problems as well. Therefore, shape optimization has been intensively studied in the literature, see [22, 27, 30, 33], and the references therein. Especially, the development of efficient algorithms in shape optimization is of growing interest.

In [10]–[16], the authors considered the numerical solution of several elliptic shape optimization problems. A boundary variational approach was proposed in combination with boundary integral representations of the shape gradient and the shape Hessian. The considered class of model problems allowed the use of boundary integral methods to compute all ingredients of the functional, the gradient, and the Hessian, which arise from the state equation. In combination with a fast wavelet Galerkin method to solve the boundary integral equations, we gained very efficient first and second order algorithms for shape problems in two and three space dimensions. In particular, the use of boundary element methods requires only a discretization of the free boundary. To our opinion this is very advantageous since on the one hand, boundary integral methods reduce the complexity, on the other hand, arbitrary deformations of the domains are realizable without any remeshing. Nevertheless, pure boundary integral methods are limited to a small class of shape optimization problems, see [11] for details. Therefore, the present paper is intended to extend our ideas to more general shape functionals.

1. Motivation and Background

Let $\Omega \in \mathbb{R}^n$, $n = 2, 3$, be a simply connected domain with boundary $\Gamma := \partial\Omega$ and assume a compact set $B \subset \Omega$, see also Figure 1.1. In the present paper we shall consider the

following shape optimization problem

$$J(\Omega) = \int_B j\big(u(\mathbf{x}), \mathbf{x}\big) d\mathbf{x} \to \min, \tag{1.1}$$

where the state u satisfies the boundary value problem

$$\begin{aligned} -\Delta u &= f \qquad \text{in } \Omega, \\ u &= g \qquad \text{on } \Gamma. \end{aligned} \tag{1.2}$$

We suppose $j \in C^2(\mathbb{R} \times B)$ and $f \in C^{0,\alpha}(D), g \in C^{2,\alpha}(D)$ for some $\alpha \in (0,1)$, where $D \supset \Omega$ denotes the hold all.

Following [8, 9], the directional derivative with respect to a sufficiently smooth domain or boundary perturbation field $\mathbf{V}$ reads as

$$\nabla J(\Omega)[\mathbf{V}] = \int_\Gamma \langle \mathbf{V}, \mathbf{n} \rangle \frac{\partial (g-u)}{\partial \mathbf{n}} \frac{\partial p}{\partial \mathbf{n}} d\sigma_{\mathbf{x}}. \tag{1.3}$$

Herein, the function p indicates the adjoint state which satisfies the boundary value problem

$$\begin{aligned} -\Delta p &= \chi_B \cdot \frac{\partial j}{\partial u}\big(u(\cdot), \cdot\big) \qquad \text{in } \Omega, \\ p &= 0 \qquad\qquad\qquad\qquad\quad \text{on } \Gamma, \end{aligned} \tag{1.4}$$

where χ_B denotes the characteristic function of B, i.e. $\chi_B = 1$ on B and $\chi_B = 0$ on $\mathbb{R}^n \setminus B$. Especially in the important case of $L^2(B)$-tracking type functionals, that is

$$j\big(u(\mathbf{x}), \mathbf{x}\big) \equiv \frac{1}{2}\big(u(\mathbf{x}) - u_0(\mathbf{x})\big)^2 \quad \text{on } B,$$

where u_0 is a given function, we observe that the adjoint state depends on the actual state u because of

$$\frac{\partial j}{\partial u}\big(u(\cdot), \cdot\big) = u - u_0 \quad \text{on } B.$$

Consequently, a numerical method for solving the state equation (1.2) should provide a fast access to u in the set B, like finite element methods. However, we like to preserve the advantages of boundary integral methods to treat the free boundary Γ. This suggests to couple finite element methods and boundary integral methods in order to compute the state and its adjoint.

The paper is organized as follows. In Section 2 we analyze the problem under consideration. In particular, we prove that the shape Hessian of the functional (1.1) is compact, which shows that the shape optimization problem is *ill-posed*. According to [17], we cannot expect convergence of a Ritz-Galerkin solution to the optimal domain since local convexity is missing. In Section 3 we consider the efficient solution of the state equation (1.2) and its adjoint (1.4) by the coupling of FEM and BEM. Finally, in Section 4 we carry out numerical tests which confirm that we succeeded in finding a fast method to solve the considered class of shape optimization problems. However, the results also indicate the ill-posedness of the optimization problem under consideration.

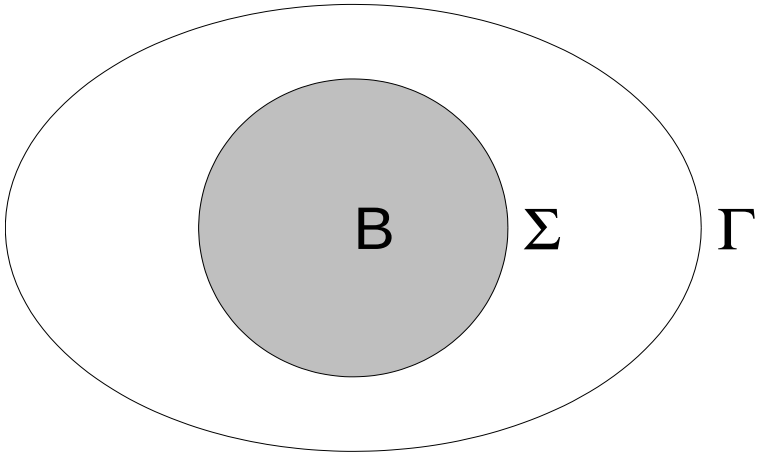

FIGURE 1.1. The domain Ω, the compact set B, and the boundaries Γ and Σ.

In the following, in order to avoid the repeated use of generic but unspecified constants, by $C \lesssim D$ we mean that C can be bounded by a multiple of D, independently of parameters which C and D may depend on. Obviously, $C \gtrsim D$ is defined as $D \lesssim C$, and $C \sim D$ as $C \lesssim D$ and $C \gtrsim D$.

2. Analysing the Shape Optimization Problem

2.1. **Shape Calculus.** We shall focus first on the shape calculus via boundary variations. For a general overview on shape calculus, mainly based on the perturbation of identity (Murat and Simon) or the speed method (Sokolowski and Zolesio), we refer the reader for example to Murat and Simon [29, 32], Pironneau [30], Sokolowski and Zolesio [33], Delfour and Zolesio [7], and the references therein.

We introduce the following notation. The unit sphere in $\mathbb{R}^n$ will be denoted by

$$\mathbb{S} := \{\widehat{\mathbf{x}} \in \mathbb{R}^n : \|\widehat{\mathbf{x}}\| = 1\}.$$

Here and in the sequel, $\widehat{\mathbf{x}}$ indicates always a point on the unit sphere. In particluar, for a point $\mathbf{x} \in \mathbb{R}^n$ the notion $\widehat{\mathbf{x}}$ has to be understood as $\widehat{\mathbf{x}} := \mathbf{x}/\|\mathbf{x}\|$.

Next, we adopt the shape calculus from [8, 9] to our model problem. Note that we have to assume $\Omega \in C^{2,\alpha}$ for some fixed $\alpha \in (0,1)$ for the second order boundary perturbation calculus, in contrast to $\Omega \in C^2$ for the first order calculus. For sake of simplicity, we suppose the domain Ω to be star-shaped. Then, we can identify it with a function, that describes its boundary Γ, i.e., we have

$$\Gamma := \{r(\widehat{\mathbf{x}}) \cdot \widehat{\mathbf{x}} : \widehat{\mathbf{x}} \in \mathbb{S}\},$$

where $r \in C^{2,\alpha}(\mathbb{S})$ is a positive function with $r \geq \delta > 0$. We introduce the function $dr \in C^{2,\alpha}(\mathbb{S})$ as standard variation for perturbed domains Ω_ε and boundaries Γ_ε, respectively, defined via

$$r_\varepsilon(\widehat{\mathbf{x}}) = r(\widehat{\mathbf{x}}) + \varepsilon dr(\widehat{\mathbf{x}}).$$

The main advantage of this approach is a complete embedding of the shape problem into a Banach space setting. That is, *both* the shapes and their increments, can be viewed as elements of $C^{2,\alpha}(\mathbb{S})$. We like to mention that, instead of the unit sphere and variations in radial direction, one may use other reference manifolds and variation fields to derive a second order Fréchet calculus.

In accordance with Section 1, we find for our particular setting the identities $\mathbf{V}(\mathbf{x}) = dr(\widehat{\mathbf{x}}) \cdot \widehat{\mathbf{x}}$ and

$$\langle \mathbf{V}, \mathbf{n} \rangle d\sigma_{\mathbf{x}} = dr(\widehat{\mathbf{x}}) \langle \widehat{\mathbf{x}}, \mathbf{n} \rangle d\sigma_{\mathbf{x}} = dr(\widehat{\mathbf{x}}) r(\widehat{\mathbf{x}})^{n-1} d\sigma_{\widehat{\mathbf{x}}} \tag{2.5}$$

for all $\mathbf{x} \in \Gamma$. Consequently, the shape gradient (1.3) becomes in spherical coordinates

$$\nabla J(\Omega)[dr] = \int_{\mathbb{S}} dr\, r^{n-1}\, \frac{\partial p}{\partial \mathbf{n}} \frac{\partial (g-u)}{\partial \mathbf{n}} d\sigma_{\widehat{\mathbf{x}}}. \tag{2.6}$$

Therefore, the boundary integral representation of the shape Hessian is given by

$$\begin{aligned} \nabla^2 J(\Omega)[dr_1, dr_2] = \int_{\mathbb{S}} dr_1 dr_2 \Bigg\{ & (n-1) r^{n-2} \frac{\partial p}{\partial \mathbf{n}} \frac{\partial (g-u)}{\partial \mathbf{n}} + r^{n-1} \frac{\partial}{\partial \widehat{\mathbf{x}}} \Big[\frac{\partial p}{\partial \mathbf{n}} \cdot \frac{\partial (g-u)}{\partial \mathbf{n}} \Big] \Bigg\} \\ & + dr_1\, r^{n-1} \Big[- \frac{\partial p}{\partial \mathbf{n}} \cdot \frac{\partial du[dr_2]}{\partial \mathbf{n}} + \frac{\partial dp[dr_2]}{\partial \mathbf{n}} \cdot \frac{\partial (g-u)}{\partial \mathbf{n}} \Big] d\sigma_{\widehat{\mathbf{x}}}. \end{aligned} \tag{2.7}$$

Herein, the notion $\partial / \partial \widehat{\mathbf{x}}$ has to be understood in the sense of $\partial u / \partial \widehat{\mathbf{x}} = \langle \nabla u, \widehat{\mathbf{x}} \rangle$. Moreover, $du = du[dr_2]$ and $dp = dp[dr_2]$ denote the local shape derivatives of the state function and the adjoint state function, which satisfy the boundary value problems

$$\begin{aligned} \Delta du &= 0 && \text{in } \Omega, \\ du &= dr_2 \langle \widehat{\mathbf{x}}, \mathbf{n} \rangle \frac{\partial (g-u)}{\partial \mathbf{n}} && \text{on } \Gamma, \end{aligned} \tag{2.8}$$

and

$$\begin{aligned} -\Delta dp &= \chi_B du[dr_2] \cdot \frac{\partial^2 j}{\partial u^2}\big(u(\cdot), \cdot\big) && \text{in } \Omega, \\ dp &= -dr_2 \langle \widehat{\mathbf{x}}, \mathbf{n} \rangle \frac{\partial p}{\partial \mathbf{n}} && \text{on } \Gamma, \end{aligned} \tag{2.9}$$

respectively, where the inhomogenity in (2.9) reduces further to $\chi_B du[dr_2]$ in the particular case of the L^2-tracking objective. Note that the shape Hessian (2.7) defines a continuous bilinear form on $H^{1/2}(\Gamma) \times H^{1/2}(\Gamma)$.

Remark 2.1. *Equivalent domain integral representations for the shape gradient and shape Hessian can be directly derived from the differentiation of* (1.1). *Precisely, we have*

$$\begin{aligned} \nabla J(\Omega)[dr] &= \int_B \frac{\partial j}{\partial u}\big(u(\mathbf{x}), \mathbf{x}\big)\, du[dr](\mathbf{x})\, d\mathbf{x}, \\ \nabla^2 J(\Omega)[dr_1, dr_2] &= \int_B \frac{\partial^2 j}{\partial u^2}\big(u(\mathbf{x}), \mathbf{x}\big)\, du[dr_1](\mathbf{x})\, du[dr_2](\mathbf{x})\, d\mathbf{x} \\ &\quad + \int_B \frac{\partial j}{\partial u}\big(u(\mathbf{x}), \mathbf{x}\big)\, d^2u[dr_1, dr_2](\mathbf{x})\, d\mathbf{x}, \end{aligned} \tag{2.10}$$

where the second local derivative $d^2u = d^2u[dr_1, dr_2]$ of the state u satisfies a characterization equation similar to the first derivative

$$
\begin{aligned}
\Delta d^2u &= 0 && \text{in } \Omega,\\
d^2u &= dr_1 dr_2 \frac{\partial^2(g-u)}{\partial \widehat{\mathbf{x}}^2} - dr_1 \frac{\partial du[dr_2]}{\partial \widehat{\mathbf{x}}} - dr_2 \frac{\partial du[dr_1]}{\partial \widehat{\mathbf{x}}} && \text{on } \Gamma,
\end{aligned}
\tag{2.11}
$$

see [8]. *Especially, symmetry of the shape Hessian can be seen clearly. Moreover, in case of compactly supported objectives, the local derivatives du provide a complete functional analytical tool for proving Fréchet differentiability, cf.* [32]. *Nevertheless, we like to stress that* (2.6) *and* (2.7) *are more efficient to compute an appropriate descent direction.*

2.2. **Compactness of the Hessian at the Optimal Domain.** Next, we will investigate the shape Hessian at a stationary domain $\Omega^\star$, that is, the first order necessary condition $\nabla J(\Omega^\star)[dr] = 0$ holds for all $dr \in C^{2,\alpha}(\mathbb{S})$. Consequently, all quantities arising in the considerations below are related to the domain $\Omega^\star$. In particular, the functions u, du, etc. are the solutions of the boundary value problems (1.2), (2.8) with respect to $\Omega^\star$. Note that the necessary condition implies

$$
\frac{\partial p}{\partial \mathbf{n}} \frac{\partial (u-g)}{\partial \mathbf{n}} \equiv 0 \quad \text{on } \Gamma.
\tag{2.12}
$$

Lemma 2.2. *Equation* (2.12) *is satisfied if and only if $\partial(u-g)/\partial\mathbf{n} \equiv 0$ or $\partial p/\partial \mathbf{n} \equiv 0$ on Γ. In the latter case it follows $p \equiv 0$ in $\Omega^\star \setminus B$.*

Proof. Assume $\partial(u-g)/\partial\mathbf{n} \neq 0$ on a subset $\Phi \subset \Gamma$ with nontrivial measure. Then, it must hold $\partial p/\partial \mathbf{n} \equiv 0$ on Φ. Since p is harmonic in $\Omega^\star \setminus B$ according to (1.4) and due to the homogeneous Dirichlet boundary conditions at Γ, the unique continuation property for C^2-boundaries (cf. Hörmander [25]) implies immediately $p \equiv 0$ in $\Omega^\star \setminus B$. In particular, we conclude $\partial p/\partial \mathbf{n} \equiv 0$ on whole Γ. □

The solution $\partial(u-g)/\partial\mathbf{n} \equiv 0$ corresponds to a degeneration of the data and of the whole shape problem, respectively, and makes no sense. Especially, it would imply $du[dr] \equiv 0$ for all admissible dr according to (2.8). Thus, we suppose $\partial p/\partial \mathbf{n} \equiv 0$. Then, since $p \equiv 0$ in $\Omega^\star \setminus B$, the shape Hessian simplifies to

$$
\nabla^2 J(\Omega^\star)[dr_1, dr_2] = \int_{\mathbb{S}} dr_1\, r^{n-1} \frac{\partial dp[dr_2]}{\partial \mathbf{n}} \cdot \frac{\partial (g-u)}{\partial \mathbf{n}}\, d\sigma_{\widehat{\mathbf{x}}},
\tag{2.13}
$$

where the adjoint local shape derivative $dp = dp[dr_2]$ satisfies

$$
\begin{aligned}
-\Delta dp &= \chi_B du[dr_2] \cdot \frac{\partial^2 j}{\partial u^2}\big(u(\cdot),\cdot\big) && \text{in } \Omega^\star,\\
dp &= 0 && \text{on } \Gamma.
\end{aligned}
\tag{2.14}
$$

The next result is derived as an immediate consequence of the identities (2.10).

Lemma 2.3. *Suppose $\partial(u-g)/\partial\mathbf{n} \neq 0$ almost everywhere on Γ and $\partial^2 j/\partial u^2\big(u(\cdot),\cdot\big) \neq 0$ nonnegative on B. Then, the shape Hessian $\nabla^2 J(\Omega^\star)$ is a positive bilinear form, i.e.,*

$$
\nabla^2 J(\Omega^\star)[dr, dr] > 0
$$

for all admissible dr.

Proof. We show first that the second term of the domain representation of the shape Hessian in (2.10) vanishes at $\Omega^\star$, that is

$$\int_B \frac{\partial j}{\partial u}\big(u(\mathbf{x}),\mathbf{x}\big)\, d^2u[dr,dr]\, d\mathbf{x} = 0 \tag{2.15}$$

for all admissible dr. Using (1.4), the following transformation is obvious

$$\begin{aligned}\int_B \frac{\partial j}{\partial u}\big(u(\mathbf{x}),\mathbf{x}\big)\, d^2u[dr,dr](\mathbf{x})\, d\mathbf{x} &= -\int_B \Delta p\, d^2u[dr,dr](\mathbf{x})\, d\mathbf{x}\\ &= \int_\Gamma \frac{\partial p}{\partial \mathbf{n}}\, d^2u[dr,dr](\mathbf{x})\, d\sigma_{\mathbf{x}}.\end{aligned}$$

Hence, (2.15) follows immediately from $\partial p/\partial \mathbf{n}$ in accordance with Lemma 2.2. Consequently, we arrive at the identity

$$\nabla^2 J(\Omega^\star)[dr,dr] = \int_B \frac{\partial^2 j}{\partial u^2}\big(u(\mathbf{x}),\mathbf{x}\big)\,\big(du[dr](\mathbf{x})\big)^2\, d\mathbf{x}.$$

Observing that $du[dr]$ is a harmonic function, we conclude that $du[dr] \neq 0$ almost everywhere in B provided that $dr \not\equiv 0$ on Γ. This implies the assertion. □

We emphasize that the domain $\Omega^\star$ is only a regular strict minimizer of second order if the shape Hessian is *strictly* $H^{1/2}(\Gamma)$-coercive, that is $\nabla^2 J(\Omega^\star)[dr,dr] \geq c\|dr\|^2_{H^{1/2}(\Gamma)}$, cf. [3, 4, 17]. Consequently, the positivity of $\nabla^2 J(\Omega^\star)$ in the case of the quadratic tracking objective (if $\partial(u-g)/\partial\mathbf{n} \neq 0$ almost everywhere on Γ) is only a necessary but *not* a sufficient second order condition. We will show next that the shape Hessian is compact which immediately implies that strict $H^{1/2}(\Gamma)$-coercivity cannot be satisfied for the general class of objectives under consideration.

Lemma 2.4. *The multiplication operator*

$$M : H^{1/2}(\Gamma) \to H^{1/2}(\Gamma), \qquad Mdr := dr \cdot \langle \widehat{\mathbf{x}}, \mathbf{n}\rangle \frac{\partial(g-u)}{\partial \mathbf{n}} \tag{2.16}$$

is continuous.

Proof. Abbreviating $\omega := \langle \widehat{\mathbf{x}}, \mathbf{n}\rangle \partial(g-u)/\partial\mathbf{n}$ we may write $Mdr = dr\cdot\omega$. Due to results of Triebel [34] or Mazja and Shaposhnikova [28], the multiplication operator M is continuous from $H^{1/2}(\Gamma)$ to $H^{1/2}(\Gamma)$ if $\omega \in C^{0,\alpha}(\Gamma)$ for some $\alpha > 1/2$. Due to our assumptions on the data and the regularity of the admissible domains the latter condition holds. □

Lemma 2.5. *The mapping*

$$\Lambda : H^{1/2}(\Gamma) \to H^{-1/2}(\Gamma), \quad \Lambda(Mdr) = \frac{\partial dp[dr]}{\partial \mathbf{n}},$$

that maps $Mdr \in H^{1/2}(\Gamma)$ via (2.8) and (2.14) onto the Neumann data $\partial dp[dr]/\partial\mathbf{n} \in H^{-1/2}(\Gamma)$ of the adjoint local shape derivative, is compact.

Proof. It is well known, that the Dirichlet-to-Neumann map $\mathcal{A} : H^{1/2}(\Gamma) \to H^{-1/2}(\Gamma)$ maps the given Dirichlet data $du[dr]|_\Gamma = Mdr \in H^{1/2}(\Gamma)$ continuously to the Neumann data $\partial du[dr]/\partial \mathbf{n} = \mathcal{A}(Mdr) \in H^{-1/2}(\Gamma)$. Green's representation formula yields

$$du[dr](\mathbf{x}) = \int_\Gamma E(\mathbf{x},\mathbf{y}) \frac{\partial du[dr]}{\partial \mathbf{n}}(\mathbf{y}) d\sigma_\mathbf{y} - \int_\Gamma \frac{\partial}{\partial \mathbf{n}} E(\mathbf{x},\mathbf{y}) du[dr](\mathbf{y}) d\sigma_\mathbf{y}, \quad \mathbf{x} \in \Omega^\star,$$

where the fundamental solution $E(\mathbf{x},\mathbf{y})$ is given by

$$E(\mathbf{x},\mathbf{y}) = \begin{cases} -\frac{1}{2\pi} \log \|\mathbf{x}-\mathbf{y}\|, & \text{if } n = 2, \\ \frac{1}{4\pi \|\mathbf{x}-\mathbf{y}\|}, & \text{if } n = 3. \end{cases} \tag{2.17}$$

We denote by $\boldsymbol{\alpha} = (\alpha_1, \ldots, \alpha_n)$ multi-indices of dimension n and define $|\alpha| := \alpha_1 + \ldots + \alpha_n$. Since $\operatorname{dist}(\mathbf{B}, \Gamma) > 0$, one readily infers that differentiation gives

$$\partial_\mathbf{x}^{\boldsymbol{\alpha}} du[dr](\mathbf{x}) = \int_\Gamma \partial_\mathbf{x}^{\boldsymbol{\alpha}} E(\mathbf{x},\mathbf{y}) \frac{\partial du[dr]}{\partial \mathbf{n}}(\mathbf{y}) d\sigma_\mathbf{y} - \int_\Gamma \frac{\partial}{\partial \mathbf{n}_\mathbf{y}} \partial_\mathbf{x}^{\boldsymbol{\alpha}} E(\mathbf{x},\mathbf{y}) du[dr](\mathbf{y}) d\sigma_\mathbf{y},$$

where the kernel $\partial_\mathbf{x}^\alpha E(\mathbf{x},\cdot)$ keeps still bounded in $H^{1/2}(\Gamma)$ for all $\mathbf{x} \in B$ and $|\boldsymbol{\alpha}| \in \mathbb{N}$. Hence, we arrive at

$$\begin{aligned} \|\partial_\mathbf{x}^{\boldsymbol{\alpha}} du[dr]\|_{L^\infty(B)} &\lesssim \max_{\mathbf{x}\in\mathbf{B}} \|\partial_\mathbf{x}^{\boldsymbol{\alpha}} E(\mathbf{x},\cdot)\|_{H^{1/2}(\Gamma)} \big(\|\mathcal{A}(Mdr)\|_{H^{-1/2}(\Gamma)} + \|Mdr\|_{H^{1/2}(\Gamma)} \big) \\ &\lesssim \|Mdr\|_{H^{1/2}(\Gamma)}, \end{aligned}$$

which immediately implies the compactness of

$$\mathcal{B} : H^{1/2}(\Gamma) \to H^{-1}(\Omega^\star), \quad \mathcal{B}(Mdr) = \chi_B du[dr] \cdot \frac{\partial^2 j}{\partial u^2}\big(u(\cdot),\cdot\big).$$

Next, since the solution operator $\mathcal{C} : H^{-1}(\Omega^\star) \to H^1(\Omega^\star)$ of the Poisson equation $\Delta q = f$ in $\Omega^\star$ with homogeneous Dirichlet data $q|_\Gamma = 0$, that maps the inhomogenity $f \in H^{-1}(\Omega^\star)$ onto the solution $q \in H^1(\Omega^\star)$, is continuous, one readily infers that the mapping

$$\mathcal{D} : H^{-1}(\Omega^\star) \to H^{-1/2}(\Gamma), \quad \mathcal{D}(f) = \frac{\partial q}{\partial \mathbf{n}}$$

is continuous. Using now the identity

$$\Lambda(Mdr) = (\mathcal{D} \circ \mathcal{B})(Mdr)$$

leads to the desired result. □

Invoking (2.5), the shape Hessian (2.13) defines the following continuous bilinear form on $H^{1/2}(\Gamma) \times H^{1/2}(\Gamma)$

$$\nabla^2 J(\Omega^\star)[dr_1, dr_2] = \big(Mdr_1, \Lambda(Mdr_2)\big)_{L^2(\Gamma)}. \tag{2.18}$$

According to the Lemmata 2.4 and 2.5 we conclude the final result.

Proposition 2.6. *The shape Hessian*

$$\mathcal{H} : H^{1/2}(\Gamma) \to H^{-1/2}(\Gamma), \quad \mathcal{H} = M^\star \Lambda M : H^{1/2}(\Gamma) \to H^{-1/2}(\Gamma),$$

is compact at the optimal domain $\Omega^\star$.

Remark 2.7. *Assuming the boundaries Γ and ∂B as well as all data to be arbitrary smooth, one readily infers that the shape Hessian is even compact as mapping $\mathcal{H} : H^s(\Gamma) \to H^{-s}(\Gamma)$ for all $s > 1/2$. In this case, the eigenvalues of the Hessian decrease exponentially, as observed in the numerical example presented in Section 4.*

Proposition 2.6 implies the ill-posedness of the optimization problem itself, which is completely characterized by the nature of the shape Hessian at the critical domain.

2.3. **Ritz-Galerkin Approximation of the Shape Problem.** In order to solve the minimization problem defined by (1.1) and (1.2), we are looking for the stationary points $\Omega^\star$ satisfying

$$\nabla J(\Omega^\star)[dr] = 0 \quad \text{for all } dr \in C^{2,\alpha}(\mathbb{S}). \tag{2.19}$$

In accordance with [17] we shall introduce a Ritz-Galerkin method for the nonlinear equation (2.19). To this end, we restrict ourselves again to star-shaped domains and consider the gradient in terms of sphericals coordinates (2.6). Nevertheless, one can consider any fixed variation field with respect to a smooth reference manifold as well, see [17] for the details.

Let $\phi_1, \phi_2, \ldots, \phi_N$ denote the first N spherical harmonics in $\mathbb{R}^n$ and consider the ansatz space

$$V_N = \operatorname{span}\{\phi_1, \phi_2, \ldots, \phi_N\} \subset C^{2,\alpha}(\mathbb{S}).$$

We identify the (finite dimensional) domain Ω_N with the radial function

$$r_N(\widehat{\mathbf{x}}) = \sum_{n=0}^{N} a_n \phi_n(\widehat{\mathbf{x}}), \quad \widehat{\mathbf{x}} \in \mathbb{S}.$$

Then, we can replace (2.19) by its finite dimensional counterpart:

$$\text{seek } r_N^\star \in V_N \text{ such that } \quad \nabla J(r_N^\star)[dr] = 0 \quad \text{for all } dr \in V_N. \tag{2.20}$$

Note that this is the necessary condition associated with the finite dimensional optimization problem

$$J(r_N) \to \min, \quad r_N \in V_N. \tag{2.21}$$

According to [17] we obtain an approximation error that stays in the energy norm $H^{1/2}(\mathbb{S})$ proportional to the best approximation in V_N, that is

$$\|r_N^\star - r^\star\|_{H^{1/2}(\mathbb{S})} \lesssim \inf_{r_N \in V_N} \|r_N - r^\star\|_{H^{1/2}(\mathbb{S})},$$

provided that the shape Hessian is *strictly* $H^{1/2}(\Gamma)$-coercive at the optimal domain $\Omega^\star$. Since this is not the case as proven in the previous subsection, we cannot guarantee convergence of the solution of (2.21) to the solution $r^\star$ of the original shape optimization problem (1.1). This will be confirmed by our numerical results, see Section 4.

3. Numerical Method to compute the State and its Adjoint

3.1. **Reformulation of the State Equation.** During an iterative optimization process, we have to solve the boundary value problems (1.2) and (1.4) in each step. We emphasize that the underlying domains are always different. Finite element methods suffer from generating a suitable triangulation for each new domain. One way out is to reformulate the given boundary value problems as coupled problems involving only boundary integral equations on the free boundary. In order to perform this reformulation, we introduce a Newton potential N_f satisfying

$$-\Delta N_f = f \qquad \text{in } \widehat{\Omega}, \tag{3.22}$$

to resolve the inhomogenity in the state equation (1.2). Herein, $\widehat{\Omega}$ is a sufficiently large domain containing all domains from the iteration process. This Newton potential is supposed to be explicitly known like in our numerical example (see Section 4) or computed with sufficiently high accuracy. Such an idea has been proposed for example by Jung and Steinbach [26]. We emphasize that the Newton potential has to be computed only once in advance.

For a first order optimization method, we require the Newton potential itself as well as its gradient. Therefore, one can compute it by usual lowest order finite elements. However, since the domain $\widehat{\Omega}$ can be chosen fairly simple, one can also use e.g. finite elements based on tensor products of higher order B-splines (in $[-R,R]^n$) or dual reciprocity methods. The ansatz

$$u = N_f + v \tag{3.23}$$

yields then the problem of seeking a harmonic function v satisfying the following Dirichlet problem for the Laplacian

$$\begin{aligned} \Delta v &= 0 && \text{in } \Omega, \\ v &= g - N_f && \text{on } \Gamma. \end{aligned} \tag{3.24}$$

Now, we are able to compute both, the state and the adjoint state, by the method proposed in the next subsection.

3.2. **The Coupling of FEM and BEM.** In view of (1.4) and (3.24) we shall provide a method to solve

$$\begin{aligned} -\Delta u &= f && \text{in } B, \\ \Delta u &= 0 && \text{in } \Omega \setminus B, \\ u &= g && \text{on } \Gamma. \end{aligned} \tag{3.25}$$

We set $\Sigma := \partial B$ and assume the normal vectors $\mathbf{n}$ at Γ and Σ to point into $\Omega \setminus B$, cf. Figure 1.1 for the topological situation. Then, (3.25) can be split in two coupled

boundary value problems

$$
\begin{aligned}
-\Delta u &= f && \text{in } B,\\
\Delta u &= 0 && \text{in } \Omega \setminus B,\\
\lim_{\substack{\mathbf{y}\to\mathbf{x}\\ \mathbf{y}\in B}} u(\mathbf{y}) &= \lim_{\substack{\mathbf{y}\to\mathbf{x}\\ \mathbf{y}\in\Omega\setminus B}} u(\mathbf{y}) && \text{for all } \mathbf{x}\in\Sigma,\\
\lim_{\substack{\mathbf{y}\to\mathbf{x}\\ \mathbf{y}\in B}} \frac{\partial u}{\partial \mathbf{n}}(\mathbf{y}) &= \lim_{\substack{\mathbf{y}\to\mathbf{x}\\ \mathbf{y}\in\Omega\setminus B}} \frac{\partial u}{\partial \mathbf{n}}(\mathbf{y}) && \text{for all } \mathbf{x}\in\Sigma,\\
u &= g && \text{on } \Gamma.
\end{aligned}
\tag{3.26}
$$

We introduce the *single layer operator* $\mathcal{V}_{\Phi\Psi}$, the *double layer operator* $\mathcal{K}_{\Phi\Psi}$, the *adjoint double layer operator* $\mathcal{K}^{\star}_{\Psi\Phi}$ and the *hypersingular operator* $\mathcal{W}_{\Phi\Psi}$ with respect to the boundaries $\Phi, \Psi \in \{\Gamma, \Sigma\}$ by

$$
\begin{aligned}
(\mathcal{V}_{\Phi\Psi}u)(\mathbf{x}) &:= \int_{\Phi} E(\mathbf{x},\mathbf{y})u(\mathbf{y})d\sigma_{\mathbf{y}},\\
(\mathcal{K}_{\Phi\Psi}u)(\mathbf{x}) &:= \int_{\Phi} \frac{\partial}{\partial \mathbf{n}_{\mathbf{y}}} E(\mathbf{x},\mathbf{y})u(\mathbf{y})d\sigma_{\mathbf{y}},\\
(\mathcal{K}^{\star}_{\Phi\Psi}u)(\mathbf{x}) &:= \int_{\Phi} \frac{\partial}{\partial \mathbf{n}_{\mathbf{x}}} E(\mathbf{x},\mathbf{y})u(\mathbf{y})d\sigma_{\mathbf{y}},\\
(\mathcal{W}_{\Phi\Psi}u)(\mathbf{x}) &:= -\frac{\partial}{\partial \mathbf{n}_{\mathbf{x}}} \int_{\Phi} \frac{\partial}{\partial \mathbf{n}_{\mathbf{y}}} E(\mathbf{x},\mathbf{y})u(\mathbf{y})d\sigma_{\mathbf{y}},
\end{aligned}
\qquad \mathbf{x}\in\Psi,
$$

where the fundamental solution $E(\mathbf{x},\mathbf{y})$ is defined as in (2.17). We shall denote by $L^2(\Phi)$ the function space of all squared integrable functions on Φ with respect to the canonical inner product

$$
(u,v)_{L^2(\Phi)} = \int_{\Phi} u(\mathbf{x})v(\mathbf{x})d\sigma_{\mathbf{x}}
$$

and by $H^s(\Phi)$ ($s \in \mathbb{R}$) the corresponding Sobolev spaces. Then, in this context, the operators with respect to one boundary are continuous mappings in the spaces

$$
\begin{aligned}
\mathcal{V}_{\Phi\Phi} &: H^{-1/2}(\Phi) \to H^{1/2}(\Phi), \qquad & \mathcal{W}_{\Phi\Phi} &: H^{1/2}(\Phi) \to H^{-1/2}(\Phi),\\
\mathcal{K}_{\Phi\Phi} &: H^{1/2}(\Phi) \to H^{1/2}(\Phi), \qquad & \mathcal{K}^{\star}_{\Phi\Phi} &: H^{-1/2}(\Phi) \to H^{-1/2}(\Phi),
\end{aligned}
$$

while in the case of mixed boundaries the operators are arbitrarily smoothing compact operators.

Finally, introducing the variables $\sigma_\Sigma := (\partial u/\partial \mathbf{n})|_\Sigma$ and $\sigma_\Gamma := (\partial u/\partial \mathbf{n})|_\Gamma$, the coupled system (3.26) yields the following nonlocal boundary value problem:

Find $(u, \sigma_\Sigma, \sigma_\Gamma)$ such that

$$
\begin{aligned}
-\Delta u &= f && \text{in } B,\\
\Delta u &= 0 && \text{on } \Omega \setminus B,\\
-\mathcal{W}_{\Sigma\Sigma} u - \mathcal{W}_{\Gamma\Sigma} g + \Big(\frac{1}{2} - \mathcal{K}^\star_{\Sigma\Sigma}\Big)\sigma_\Sigma - \mathcal{K}^\star_{\Gamma\Sigma}\sigma_\Gamma &= \sigma_\Sigma && \text{on } \Sigma, \qquad (3.27)\\
\Big(\frac{1}{2} - \mathcal{K}_{\Sigma\Sigma}\Big)u - \mathcal{K}_{\Gamma\Sigma} g + \mathcal{V}_{\Sigma\Sigma}\sigma_\Sigma + \mathcal{V}_{\Gamma\Sigma}\sigma_\Gamma &= 0 && \text{on } \Sigma,\\
-\mathcal{K}_{\Sigma\Gamma} u + \Big(\frac{1}{2} - \mathcal{K}_{\Gamma\Gamma}\Big) g + \mathcal{V}_{\Sigma\Gamma}\sigma_\Sigma + \mathcal{V}_{\Gamma\Gamma}\sigma_\Gamma &= 0 && \text{on } \Gamma.
\end{aligned}
$$

This system is the so-called *two integral formulation*, which is equivalent to our original model problem (3.25), see for example [5, 23].

3.3. **The Variational Formulation.** Next, we introduce the product space $\mathcal{H} := H^1(B) \times H^{-1/2}(\Sigma) \times H^{-1/2}(\Gamma)$ equipped by the product norm

$$\|(u, \sigma_\Sigma, \sigma_\Gamma)\|^2_{\mathcal{H}} := \|u\|^2_{H^1(B)} + \|\sigma_\Sigma\|^2_{H^{-1/2}(\Sigma)} + \|\sigma_\Gamma\|^2_{H^{-1/2}(\Gamma)}$$

for all $(u, \sigma_\Sigma, \sigma_\Gamma) \in \mathcal{H}$. Further, let $a : \mathcal{H} \times \mathcal{H} \to \mathbb{R}$, be bilinear form defined by

$$
\begin{aligned}
a\big((u, \sigma_\Sigma, \sigma_\Gamma), (v, \lambda_\Sigma, \lambda_\Gamma)\big) &= \int_B \nabla u \nabla v \, d\mathbf{x}\\
&+ \left(\begin{bmatrix} v \\ \lambda_\Sigma \\ \lambda_\Gamma \end{bmatrix}, \begin{bmatrix} \mathcal{W}_{\Sigma\Sigma} & \mathcal{K}^\star_{\Sigma\Sigma} - 1/2 & \mathcal{K}^\star_{\Gamma\Sigma} \\ 1/2 - \mathcal{K}_{\Sigma\Sigma} & \mathcal{V}_{\Sigma\Sigma} & \mathcal{V}_{\Gamma\Sigma} \\ -\mathcal{K}_{\Sigma\Gamma} & \mathcal{V}_{\Sigma\Gamma} & \mathcal{V}_{\Gamma\Gamma} \end{bmatrix} \begin{bmatrix} u \\ \sigma_\Sigma \\ \sigma_\Gamma \end{bmatrix} \right)_{L^2(\Sigma)\times L^2(\Sigma)\times L^2(\Gamma)} \qquad (3.28)
\end{aligned}
$$

where the integral operators $\mathcal{V}_{\Phi\Psi}, \mathcal{K}_{\Phi\Psi}, \mathcal{K}^\star_{\Phi\Psi}, \mathcal{W}_{\Phi\Psi}$ are given as above. For sake of simplicity in representation, we omitted the trace operator in expressions like $(v, \mathcal{W}_{\Sigma\Sigma} u)_{L^2(\Sigma)}$ etc.

Introducing the linear functional $F : \mathcal{H} \to \mathbb{R}$,

$$F(v, \lambda_\Sigma, \lambda_\Gamma) = (f, v)_{L^2(B)} + \left(\begin{bmatrix} v \\ \lambda_\Sigma \\ \lambda_\Gamma \end{bmatrix}, \begin{bmatrix} -\mathcal{W}_{\Gamma\Sigma} \\ \mathcal{K}_{\Gamma\Sigma} \\ \mathcal{K}_{\Gamma\Gamma} - 1/2 \end{bmatrix} g \right)_{L^2(\Sigma)\times L^2(\Sigma)\times L^2(\Gamma)}$$

the variational formulation is given by:

Seek $(u, \sigma_\Sigma, \Sigma_\Gamma) \in \mathcal{H}$ such that

$$a((u, \sigma_\Sigma, \sigma_\Gamma), (v, \lambda_\Sigma, \lambda_\Gamma)) = F(v, \lambda_\Sigma, \lambda_\Gamma) \qquad (3.29)$$

for all $(v, \lambda_\Sigma, \lambda_\Gamma) \in \mathcal{H}$.

Lemma 3.1. *The bilinear form $a(\cdot, \cdot)$ from (3.28) satisfies the Gårding inequality*

$$a\big((u, \sigma_\Sigma, \sigma_\Gamma), (v, \sigma_\Sigma, \sigma_\Gamma)\big) + \|u\|^2_{L^2(B)} \gtrsim \|(u, \sigma_\Sigma, \sigma_\Gamma)\|^2_{\mathcal{H}}, \qquad (3.30)$$

provided that Ω has a conformal radius < 1 if $n = 2$.

Proof. From $\mathcal{K}_{\Phi\Psi} = \mathcal{K}^{\star}_{\Psi\Phi}$ we conclude $(\mathcal{K}_{\Phi\Psi}\sigma_\Phi, \sigma_\Psi)_{L^2(\Psi)} = (\mathcal{K}^{\star}_{\Psi\Phi}\sigma_\Psi, \sigma_\Phi)_{L^2(\Phi)}$. Hence, we arrive at

$$a\big((u,\sigma_\Sigma,\sigma_\Gamma),(u,\sigma_\Sigma,\sigma_\Gamma)\big) = |u|^2_{H^1(B)} + (\mathcal{W}_{\Sigma\Sigma}u,u)_{L^2(\Sigma)} + \left(\begin{bmatrix}\sigma_\Sigma\\ \sigma_\Gamma\end{bmatrix}, \begin{bmatrix}\mathcal{V}_{\Sigma\Sigma} & \mathcal{V}_{\Gamma\Sigma}\\ \mathcal{V}_{\Sigma\Gamma} & \mathcal{V}_{\Gamma\Gamma}\end{bmatrix}\begin{bmatrix}\sigma_\Sigma\\ \sigma_\Gamma\end{bmatrix}\right)_{L^2(\Sigma)\times L(\Gamma)},$$

where $|u|^2_{H^1(B)} = \int_B \|\nabla u\|^2 d\mathbf{x}$ denotes the $H^1(B)$-semi norm. Observing that the operator

$$\mathcal{V} : H^{-1/2}(\Sigma)\times H^{-1/2}(\Gamma) \to H^{1/2}(\Sigma)\times H^{1/2}(\Gamma), \qquad \mathcal{V} := \begin{bmatrix}\mathcal{V}_{\Sigma\Sigma} & \mathcal{V}_{\Gamma\Sigma}\\ \mathcal{V}_{\Sigma\Gamma} & \mathcal{V}_{\Gamma\Gamma}\end{bmatrix},$$

is positive definite, we deduce the assertion since $\|u\|^2_{H^1(B)} = \|u\|^2_{L^2(B)} + |u|^2_{H^1(B)}$ and $(\mathcal{W}_{\Sigma\Sigma}u,u)_{L^2(\Sigma)} \geq 0$. □

Lemma 3.2. *The bilinear form $a(\cdot,\cdot)$ from (3.28) is injective, provided that Ω has a conformal radius < 1 if $n = 2$.*

Proof. Assume that $(u_1,\sigma_{\Sigma 1},\sigma_{\Gamma 1}),(u_2,\sigma_{\Sigma 2},\sigma_{\Gamma 2}) \in \mathcal{H}$ solve both the coupled problem (3.26). Then, setting $(v,\lambda_\Sigma,\lambda_\Gamma) := (u_1-u_2,\sigma_{\Sigma 1}-\sigma_{\Sigma 2},\sigma_{\Gamma 1}-\sigma_{\Gamma 2}) \in \mathcal{H}$, the Gårding inequality (3.1) implies $v = const.$ and $\lambda_\Sigma = \lambda_\Gamma = 0$. Since the underlying function is harmonic in Ω and satisfies homogeneous Dirichlet boundary conditions at Γ, it follows that $const. = 0$. □

Combining Lemmata 3.1 and 3.2 yields the following theorem.

Theorem 3.3. *The variational formulation (3.29) admits a unique solution $(u,\sigma_\Sigma,\sigma_\Gamma) \in \mathcal{H}$ for all $F \in \mathcal{H}'$, provided that Ω has a conformal radius < 1 if $n = 2$.*

Proof. The bilinear form $a(\cdot,\cdot)$ is obviously continuous on $\mathcal{H}\times\mathcal{H}$ and in accordance with Lemmata 3.1 and 3.2 $\mathcal{H}$-coercive and injective. Hence, one concludes existence and uniqueness of the solution by the Riesz-Schauder theory. □

3.4. **The Galerkin Scheme.** Since the variational formulation is stable without further restrictions, the discretization is along the lines of [20, 21]. It suffices to exploit globally continuous lowest order finite elements to discretize u and piecewise constant ansatz functions to discretize σ_Σ and σ_Γ.

We first introduce a uniform triangulation of B which induces a uniform triangulation of Σ. Moreover, we need a uniform triangulation of the free boundary Γ, which we suppose to have the same mesh size as the triangulation of the domain B. For the FEM part we consider lowest order ansatz functions $\{\phi^B_k : k \in \Delta^B\}$ with respect to the given domain mesh. For the BEM part we introduce canonical piecewise constant ansatz functions $\{\psi^\Phi_k : k \in \nabla^\Phi\}$ on the underlying triangulations of the boundaries Φ ($\Phi \in \{\Sigma,\Gamma\}$). For sake of simplicity in representation, we define $\phi^\Sigma_k := \phi^B_k|_\Sigma$ ($k \in \Delta^B$), which is mostly identical to zero and coincides with canonical piecewise linear (or bilinear) functions on Σ if the trace of the finite element function ϕ^B_k is nontrivial. Moreover, we shall

introduce further the set of canonical globally continuous piecewise linear (or bilinear) Lagrange ansatz functions on the triangulation of Γ, which we indicate by $\{\phi_k^\Gamma : k \in \Delta^\Gamma\}$ ($\#\Delta^\Gamma \sim \#\nabla^\Gamma$).

Then, introducing the system matrices

$$\begin{aligned} \mathbf{A} &= \Big[(\nabla\phi_{k'}^B, \phi_k^B)_{L^2(B)}\Big]_{k,k'}, & \mathbf{W}_{\Phi\Psi} &= \Big[(\mathcal{W}_{\Phi\Psi}\phi_{k'}^\Phi, \phi_k^\Psi)_{L^2(\Psi)}\Big]_{k,k'}, \\ \mathbf{B}_\Phi &= \Big[\tfrac{1}{2}(\phi_{k'}^\Phi, \psi_{j,k}^\Phi)_{L^2(\Phi)}\Big]_{k,k'}, & \mathbf{K}_{\Phi\Psi} &= \Big[(\mathcal{K}_{\Phi\Psi}\phi_{k'}^\Phi, \phi_k^\Psi)_{L^2(\Psi)}\Big]_{k,k'}, \\ \mathbf{G}_\Phi &= \Big[(\phi_{k'}^\Phi, \phi_{j,k}^\Phi)_{L^2(\Phi)}\Big]_{k,k'}, & \mathbf{V}_{\Phi\Psi} &= \Big[(\mathcal{V}_{\Phi\Psi}\phi_{k'}^\Phi, \phi_{j,k}^\Psi)_{L^2(\Psi)}\Big]_{k,k'}, \end{aligned} \tag{3.31}$$

where again $\Phi, \Psi \in \{\Sigma, \Gamma\}$, and the data vectors

$$\mathbf{f} = \Big[(f, \phi_k^B)_{L^2(B)}\Big]_k, \qquad \mathbf{g} = \Big[(g, \phi_k^\Gamma)_{L^2(\Gamma)}\Big]_k,$$

we obtain the following linear system of equations

$$\begin{bmatrix} \mathbf{A}+\mathbf{W}_{\Sigma\Sigma} & \mathbf{K}_{\Sigma\Sigma}^T - \mathbf{B}_\Sigma^T & \mathbf{K}_{\Sigma\Gamma}^T \\ \mathbf{B}_\Sigma - \mathbf{K}_{\Sigma\Sigma} & \mathbf{V}_{\Sigma\Sigma} & \mathbf{V}_{\Gamma\Sigma} \\ -\mathbf{K}_{\Sigma\Gamma} & \mathbf{V}_{\Sigma\Gamma} & \mathbf{V}_{\Gamma\Gamma} \end{bmatrix} \begin{bmatrix} \mathbf{u} \\ \boldsymbol{\sigma}_\Sigma \\ \boldsymbol{\sigma}_\Gamma \end{bmatrix} = \begin{bmatrix} \mathbf{f} \\ \mathbf{0} \\ \mathbf{0} \end{bmatrix} + \begin{bmatrix} -\mathbf{W}_{\Sigma\Sigma} \\ \mathbf{K}_{\Gamma\Sigma} \\ \mathbf{K}_{\Gamma\Gamma} - \mathbf{B}_\Gamma \end{bmatrix} \mathbf{G}_\Gamma^{-1}\mathbf{g} \tag{3.32}$$

We mention that $\mathbf{G}_\Gamma^{-1}\mathbf{g}$ corresponds to the $L^2(\Gamma)$-othogonal projection of the given Dirichlet data $g \in H^{1/2}(\Gamma)$ onto the space of the piecewise (bi-) linears on Γ. That way, we can also apply fast boundary element techniques to the boundary integral operators on the right hand side of the linear system of equations (3.32).

Applying standard error estimates for the Galerkin scheme and employing the Aubin Nitsche trick leads to the following error estimate concerning the present discretization.

Proposition 3.4. *Let h denote the mesh size of the triangulations of B and Γ, respectively. We denote the solution of (3.29) by $(u, \sigma_\Sigma, \sigma_\Sigma)$ and the Galerkin solution by $(u_h, \sigma_{\Sigma h}, \sigma_{\Gamma h})$. Then, we have the error estimate*

$$\begin{aligned} &\|(u, \sigma_\Sigma, \sigma_\Gamma) - (u^h, \sigma_{\Sigma h}, \sigma_{\Gamma h})\|_{L^2(B)\times H^{-2}(\Sigma)\times H^{-2}(\Sigma)} \\ &\qquad \lesssim h^2\|u\|_{H^2(B)} + h^3\|\sigma_\Sigma\|_{H^1(\Gamma)} + h^3\|\sigma_\Gamma\|_{H^1(\Gamma)} \end{aligned}$$

uniformly in h.

Finally, we shall encounter some issues on the efficient solution of the linear system of equations (3.32). The complexity is governed by the BEM part since the boundary element matrices are densely populated. On the one hand, following for example [20, 21] in case of wavelet matrix compression, one can apply fast boundary element techniques to reduce this complexity such that the over-all complexity is governed by the FEM part. On the other hand, according to [21, 24], the Bramble-Pasciak-CG ([1]) provides a fast and robust iterative solver for the above saddle point system. In particular, combining a nested iteration with the Bramble-Pasciak-Xu preconditioner ([2]) for the FEM and a wavelet preconditioning ([6, 31]) for the BEM part, we derive an asymptotical optimal solver for the above system, see [21] for the details. We refer the reader to [21] for

the implementational details of a similar coupling formulation in case of wavelet matrix compression for the boundary element part.

3.5. **Error Estimates for $L^2(B)$-Tracking Type Functionals.** Recall that, in a single iteration step of the shape optimization algorithm, we use the present method in order to solve both, the state (3.24) via the ansatz (3.23) and the adjoint state (1.4). Now, we shall specify the approximation errors to the shape functional and its gradient in the important case of $L^2(B)$-tracking type functionals. For sake of simplicity we neglect approximation errors of the Newton potential N_f (3.22), i.e., we assume that it is known analytically.

Corollary 3.5. *Assume that the Newton potential N_f from* (3.22) *is given exactly. Then, in case of $L^2(B)$-tracking type functionals both, the shape functional and the shape gradient, are approximated quadratically, that is, the approximation error behaves like $\mathcal{O}(h^2)$.*

Proof. The rate of convergence with respect of the shape functional follows from

$$\begin{aligned}|J(\Omega) - J(\Omega)_h| &= \left| \int_B u^2 - u_h^2 d\mathbf{x} \right| \\ &\leq (u - u_h, u - u_h)_{L^2(B)} + 2|(u, u - u_h)_{L^2(B)}| \lesssim h^2 \|u\|^2_{H^2(B)}.\end{aligned}$$

In case of the shape gradient we abbreviate $\sigma_\Gamma := \partial(u-g)/\partial\mathbf{n}$ and $\lambda_\Gamma := \partial p/\partial\mathbf{n}$, while $\sigma_{\Gamma h}$ and $\lambda_{\Gamma h}$ denote the numerical approximations. Since the inhomogenity of the adjoint state equation (1.4) is computed consistent to the present the formulation, we obtain the same rate of convergence rate for the unknowns of the adjoint state as of the primal state. From

$$\begin{aligned}|\nabla J(\Omega)[dr] - \nabla J(\Omega)[dr]| &= \left| \int_\Gamma \langle \mathbf{V}, \mathbf{n} \rangle \{\sigma_\Gamma \lambda_\Gamma - \sigma_{\Gamma h} \lambda_{\Gamma h}\} d\sigma \right| \\ &= \left| \int_\Gamma \langle \mathbf{V}, \mathbf{n} \rangle \{(\sigma_\Gamma - \sigma_{\Gamma h})(\lambda_\Gamma - \lambda_{\Gamma h}) - \sigma_\Gamma(\lambda_\Gamma - \lambda_{\Gamma h}) - \lambda_\Gamma(\sigma_\Gamma - \sigma_{\Gamma h})\} d\sigma \right| \\ &\leq \|\langle \mathbf{V}, \mathbf{n} \rangle\|_{L^\infty(\Gamma)} (|\sigma_\Gamma - \sigma_{\Gamma h}|, |\lambda_\Gamma - \lambda_{\Gamma h}|)_{L^2(\Gamma)} + (\langle \mathbf{V}, \mathbf{n} \rangle \sigma_\Gamma, \lambda_\Gamma - \lambda_{\Gamma h})_{L^2(\Gamma)} \\ &\qquad + (\langle \mathbf{V}, \mathbf{n} \rangle \lambda_\Gamma, \sigma_\Gamma - \sigma_{\Gamma h})_{L^2(\Gamma)}\end{aligned}$$

Herein, the first term is estimated by

$$\begin{aligned}(|\sigma_\Gamma - \sigma_{\Gamma h}|, |\lambda_\Gamma - \lambda_{\Gamma h}|)_{L^2(\Gamma)} &\leq \|\sigma_\Gamma - \sigma_{\Gamma h}\|_{L^2(\Gamma)} \|\lambda_\Gamma - \lambda_{\Gamma h}\|_{L^2(\Gamma)} \\ &\lesssim h^2 \|\sigma_\Gamma\|_{H^1(\Gamma)} \|\lambda_\Gamma\|_{H^1(\Gamma)}.\end{aligned}$$

The second term yields

$$(\langle \mathbf{V}, \mathbf{n} \rangle \sigma_\Gamma, \lambda_\Gamma - \lambda_{\Gamma h})_{L^2(\Gamma)} \leq \|\langle \mathbf{V}, \mathbf{n} \rangle \sigma_\Gamma\|_{H^1(\Gamma)} \|\lambda_\Gamma - \lambda_{\Gamma h}\|_{H^{-1}(\Gamma)} \lesssim h^2 \|\lambda_\Gamma\|_{H^1(\Gamma)}$$

and likewise the third term, which finishes the proof. □

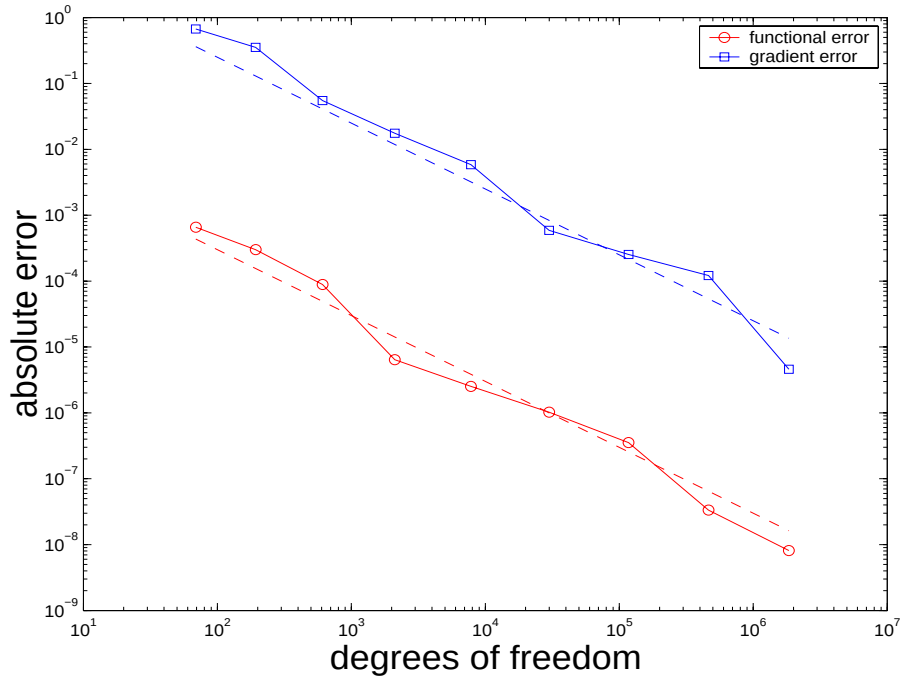

FIGURE 4.2. Degrees of freedom versus approximation error.

4. Numerical Results

The numerical example will be carried out in two space dimensions where $B = \{(x, y) : x^2 + y^2 < 0.2\}$. We consider the minimization of a $L^2(B)$-tracking type functional, precisely

$$J(\Omega) = \int_B \|u - u_0\|^2 d\mathbf{x} \to \min,$$

where u satisfies the Poisson equation $-\Delta u = 10 \cdot (2/h_x^2 + 2/h_y^2)$ in Ω with homogeneous Dirichlet data $u|_\Gamma = 0$. Herein, $h_x, h_y > 0$ are some fixed constants to be specified below. The function u_0 is chosen as

$$u_0(x, y) := 10 \cdot \left(1 - \frac{x^2}{h_x^2} - \frac{y^2}{h_y^2}\right),$$

Since $-\Delta u_0 = 20 \cdot (1/h_x^2 + 1/h_y^2)$ and $u_0 \equiv 0$ on the boundary of ellipse E with semi-axes h_x and h_y, that is

$$E := \left\{(x, y) \in \mathbb{R}^2 : \frac{x^2}{h_x^2} + \frac{y^2}{h_y^2} = 1\right\},$$

one infers that the minimizer of the considered shape problem is the ellipse E. For the present state equation we will exploit the Newton potential

$$N_f = -5 \cdot \left(\frac{1}{h_x^2} + \frac{1}{h_y^2}\right) \cdot (x^2 + y^2).$$

First, we want to check the orders of convergence predicted in Corollary 3.5. We choose $h_y = 0.4$ and $h_x = 0.6$ and compute the shape functional and its discretized gradient for a randomly chosen boundary Γ on a very fine discretization. Then, we compute on lower levels the approximate solutions und measure the absolute (ℓ^2-) errors to our reference values. The results are depicted in Figure 4.2. In fact, one observes quadratic approximation orders (indicated by the dashed lines) of both, the functional and its gradient.

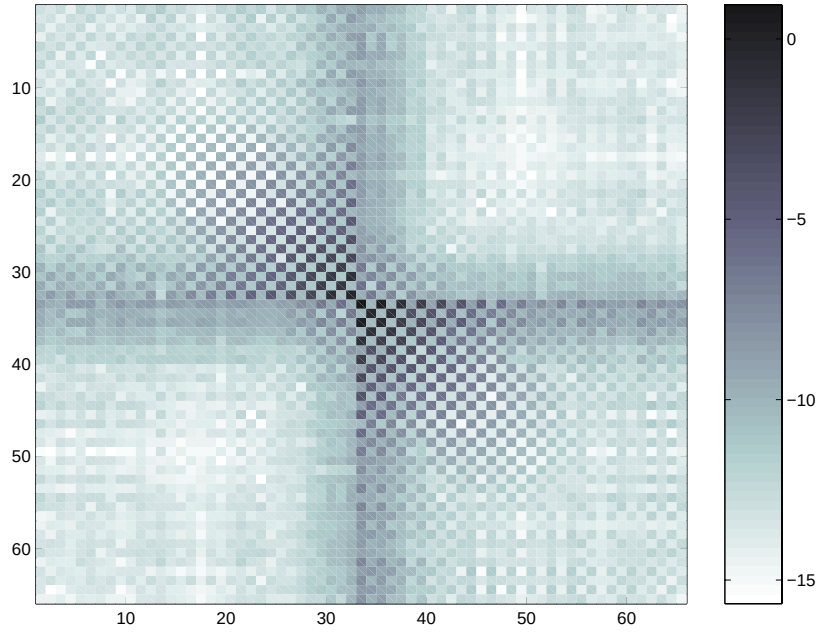

FIGURE 4.3. Logarithmic moduli of the coefficients of the discrete Hessian $d^2J(\Omega^\star)[dr_1, dr_2]$.

Next, we consider the shape Hessian (2.13) at the optimal domain $\Omega^\star$ in case of $h_x = 0.4$ and $h_y = 0.3$. It holds $\partial(u-g)/\partial\mathbf{n} > 0$ on Γ which implies in fact $\nabla^2 J(\Omega^\star)[dr, dr] > 0$ for all directions dr, see Lemma 2.3. We discretize the Hessian $\nabla^2 J(\Omega^\star)[dr_1, dr_2]$ via the first 65 $H^{1/2}$-normalized Fourier frequencies, 115201 finite elements and 1024 boundary elements each on the boundaries Σ and Γ. The underlying triangulation of B on level 2, based on Zlámal's curved finite elements [36], can be found in Figure 4.5. In Figure 4.3 we visualized the Hessian where we used the numbering $\phi_1 = \cos(32 \cdot 2\pi)/\sqrt{32}, \phi_2 = \cos(31 \cdot 2\pi)/\sqrt{31}, \ldots, \phi_{32} = \cos(2\pi), \phi_{33} = 1/\sqrt{(2\pi)}, \phi_{34} = \sin(2\pi), \ldots, \phi_{64} = \sin(31 \cdot 2\pi)/\sqrt{31}, \phi_{65} = \sin(32 \cdot 2\pi)/\sqrt{32}$. A plot of its eigenvalue distribution can be found in Figure 4.4. The plot exhibits clearly an exponential decay of the first 25 eigenvalues. The moduli of the other eigenvalues are than 10^{-11} and are not reliable due to round-off erros. Note that the ℓ^2-condition number of this discrete Hessian is about 10^{15}.

Finally, we compute the free boundary Γ in case of $h_y = 0.4$ and $h_x = 0.4, 0.5, \ldots, 1.0$ using like above the first 65 Fourier frequencies, 115201 finite elements and 1024 boundary

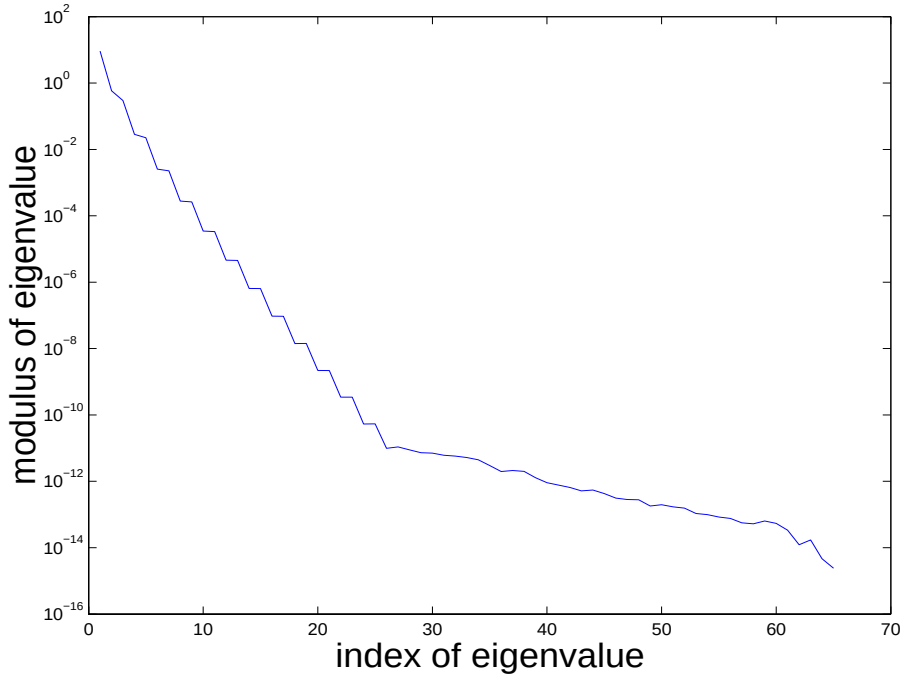

FIGURE 4.4. The eigenvalues of the discrete Hessian.

h_x	h_y	$H^{1/2}(\mathbb{S})$-shape error	cpu-time
0.4	0.4	8.4e-5	618
0.5	0.4	3.8e-2	696
0.6	0.4	1.6e-1	706
0.7	0.4	2.9e-1	687
0.8	0.4	5.2e-1	697
0.9	0.4	7.5e-1	680
1.0	0.4	1.0	708

TABLE 4.1. Approximation errors of the shape and over-all computing times.

elements each on the boundaries Σ and Γ. We employ a quasi-Newton method with quadratic line search, updated by the inverse BFGS-rule without damping, to solve the necessary condition (2.20), see e.g. [18, 19] for the details. We choose always the circle centered in $(x, y) = (0, 0)$ with radius 0.75 as initial guess and perform 50 quasi-Newton iterations.

In Table 4.1 we listed the $H^{1/2}(\mathbb{S})$-error of the final shape and the over-all cpu-times (measured in seconds), which is always about 10 minutes. From the increasing shape errors we conclude that the shape problem becomes more and more ill-posed when h_x increases. This is quite obvious since the domain Ω becomes larger.

The resulting free boundaries are plotted in Figure 4.5. The boundary increases when h_x increases. Therefore, the inner boundary corresponds to the problem with $h_x = 0.4$ while

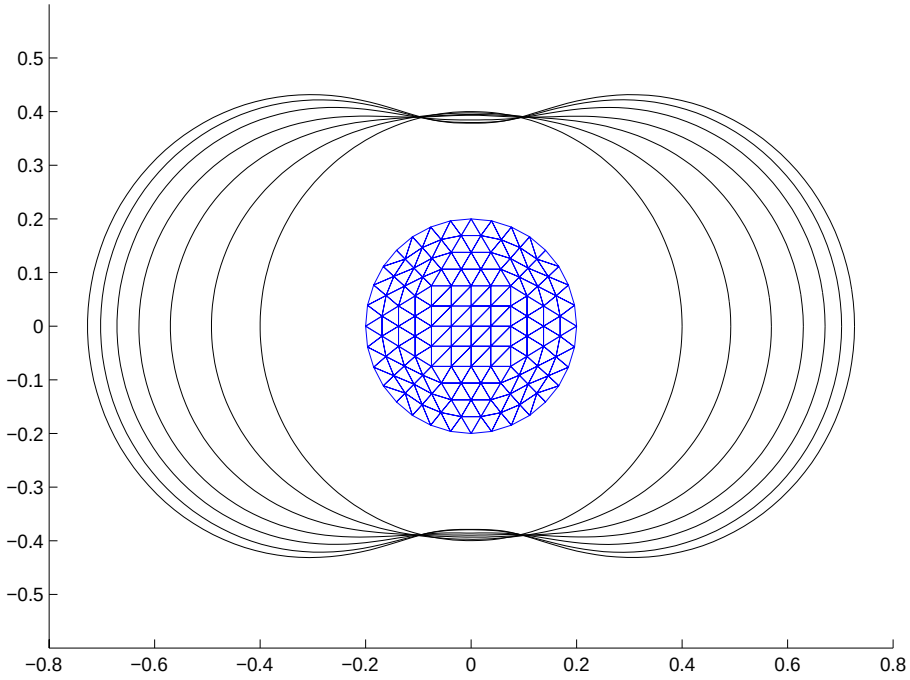

FIGURE 4.5. Computed free boundaries.

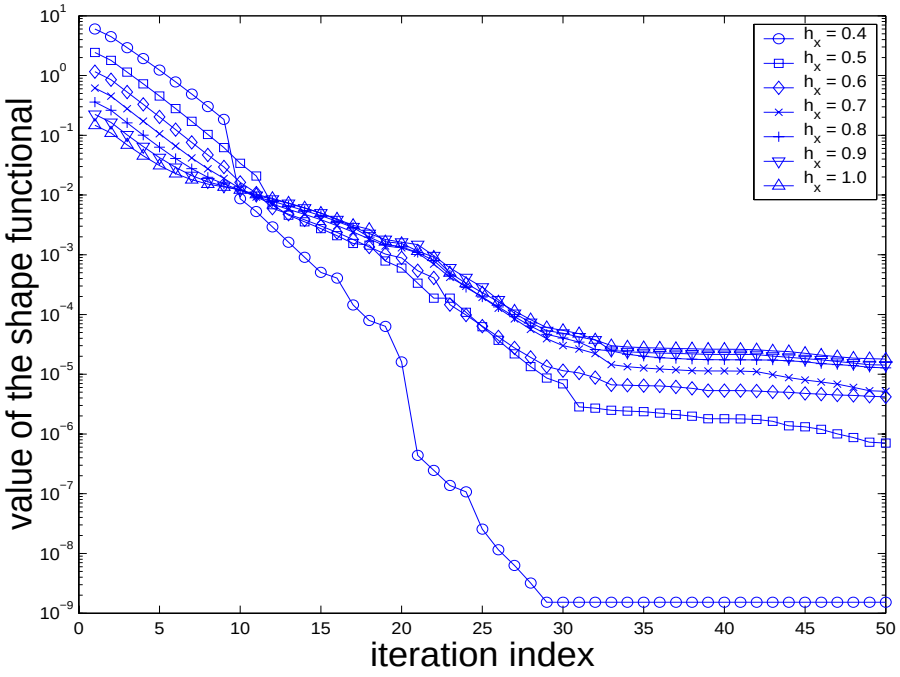

FIGURE 4.6. Histories of the shape functional.

the outer boundary corresponds to $h_x = 1.0$. Especially, we see that the computed free boundaries are only approximately ellipses.

The histories of the shape functional are plotted in Figure 4.6. For the initial gues we have $J(r_N) = 6.79519$. Except in the case of a circle ($h_x = h_y = 0.4$), where the shape optimization algorithm finds the optimal solution quite exact, seen by $J(r_N^\star) \leq 1e-9$, the curves are similar. After 50 iteration steps we have reduced the shape functional in all cases by at least five magnitudes, i.e., by a factor greater than 100 000.

References

[1] J. Bramble and J.E. Pasciak. A preconditioner technique for indefinite systems resulting from mixed approximation of elliptic problems. *Mathematics of Computation*, 50:1–17, 1988.

[2] J. Bramble, J.E. Pasciak, and J. Xu. Parallel multilevel preconditioners. *Mathematics of Computation*, 55:1–22, 1990.

[3] M. Dambrine and M. Pierre. About stability of equilibrium shapes. *M2AN* 34, No.4, 811–834, 2000.

[4] M. Dambrine. On variations of the shape Hessian and sufficient conditions for the stability of critical shapes. *RACSAM, Rev. R. Acad. Cien. Serie A. Mat.* 96, No.1, 95–121, 2002.

[5] M. Costabel and E.P. Stephan. Coupling of finite element and boundary element methods for an elasto-plastic interface problem. *SIAM Journal on Numerical Analysis*, 27:1212–1226, 1988.

[6] W. Dahmen and A. Kunoth. Multilevel preconditioning. *Numer. Math.*, 63:315–344, 1992.

[7] M. Delfour and J.-P. Zolesio. *Shapes and Geometries*. SIAM, Philadelphia, 2001.

[8] K. Eppler. Boundary integral representations of second derivatives in shape optimization. *Discussiones Mathematicae (Differential Inclusion Control and Optimization)*, 20:63–78, 2000.

[9] K. Eppler. Optimal shape design for elliptic equations via BIE-methods. *J. of Applied Mathematics and Computer Science*, 10:487–516, 2000.

[10] K. Eppler and H. Harbrecht. Numerical solution of elliptic shape optimization problems using wavelet-based BEM. *Optim. Methods Softw.*, 18:105-123, 2003.

[11] K. Eppler and H. Harbrecht. 2nd Order Shape Optimization using Wavelet BEM. *Preprint 06-2003, TU Berlin*, 2003. to appear in Optim. Methods Softw.

[12] K. Eppler and H. Harbrecht. Exterior Electromagnetic Shaping using Wavelet BEM. *Technical Report 13-2003, Math. Meth. Appl. Sci.* 28:387–405 (2005).

[13] K. Eppler and H. Harbrecht. Fast wavelet BEM for 3d electromagnetic shaping. *Bericht 03-9*, Berichtsreihe des Mathematischen Seminars der Christian-Albrechts-Universit zu Kiel, 2003. to appear in Appl. Numer. Math.

[14] K. Eppler and H. Harbrecht. A regularized Newton method in electrical impedance tomography using shape Hessian information. *WIAS-Preprint No. 943*, WIAS Berlin, 2004. to appear in Control & Cybernetics.

[15] K. Eppler and H. Harbrecht. Shape optimization in 3D electrical impedance tomography. *WIAS-Preprint 963*, WIAS Berlin, 2004. submitted to Proceeding of IFIP TC 7.2 conference.

[16] K. Eppler and H. Harbrecht. Efficient treatment of stationary free boundary problems. *WIAS-Preprint 965*, WIAS Berlin, 2004. submitted to Appl. Numer. Math.

[17] K. Eppler, H. Harbrecht, and R. Schneider. Convergence in Shape Optimization. *WIAS-Preprint 1016*, WIAS Berlin, 2005. submitted to SICON.

[18] P.E. Gill, W. Murray and M.H. Wright. *Practical Optimization.* Academic Press, New York, 1981.

[19] Ch. Grossmann and J. Terno. *Numerik der Optimierung.* Teubner, Stuttgart, 1993.

[20] H. Harbrecht, F. Paiva, C. Pérez, and R. Schneider. Biorthogonal wavelet approximation for the coupling of FEM-BEM. *Numer. Math.*, 92:325–356, 2002.

[21] H. Harbrecht, F. Paiva, C. Pérez, and R. Schneider. Wavelet preconditioning for the coupling of FEM-BEM. *Numer. Linear Algebra Appl.* 3:197–222, 2003.

[22] J. Haslinger and P. Neitaanmäki. *Finite element approximation for optimal shape, material and topology design, 2nd edition.* Wiley, Chichester, 1996.

[23] H. Han. A new class of variational formulation for the coupling of finite and boundary element methos. *Journal of Computational Mathematics*, 8(3):223–232, 1990.

[24] B. Heise and M. Kuhn. Parallel solvers for linear and nonlinear exterior magnetic field problems based upon coupled FE/BE formulations. *Computing*, 56:237–258, 1996.

[25] L. Hörmander. *The analysis of Linear Partial Differential Operators.* Springer, New York, 1983-85.

[26] M. Jung and O. Steinbach. A Finite Element-Boundary Element Algorithm for Inhomogeneous Boundary Value Problems *Computing*, 68:1–17, 2002.

[27] A.M. Khludnev and J. Sokolowski. *Modelling and control in solid mechanics.* Birkhäuser, Basel, 1997.

[28] V.G. Maz'ya and T.O. Shaposhnikova. *Theory of multipliers in spaces of differentiable functions.* Pitman, Boston, 1985.(Monographs and Studies in Mathematics, 23. Pitman Advanced Publishing Program. Boston - London - Melbourne: Pitman Publishing Inc. *XIII*, 344 p. (1985))

[29] F. Murat and J. Simon. Étude de problémes d'optimal design. in *Optimization Techniques, Modeling and Optimization in the Service of Man*, edited by J. Céa, Lect. Notes Comput. Sci. 41, Springer-Verlag, Berlin, 54–62 (1976).

[30] O. Pironneau. *Optimal shape design for elliptic systems.* Springer, New York, 1983.

[31] R. Schneider. *Multiskalen- und Wavelet-Matrixkompression: Analysisbasierte Methoden zur Lösung großer vollbesetzter Gleichungssyteme.* B.G. Teubner, Stuttgart, 1998.

[32] J. Simon. Differentiation with respect to the domain in boundary value problems. *Numer. Funct. Anal. Optimization* 2:649–687, 1980.

[33] J. Sokolowski and J.-P. Zolesio. *Introduction to Shape Optimization.* Springer, Berlin, 1992.

[34] H. Triebel. *Theory of function spaces.* Birkhäuser, Basel-Boston-Stuttgart, 1983.

[35] J. Wloka. *Partial Differential Equations.* Cambridge University Press, Cambridge, 1987.

[36] A. Zenisek. *Nonlinear Elliptic and Evolution Problems and Their Finite Element Approximation.* Academic Press, London, 1990.